Aerobic Oxidation of Amines to Imines by Cesium-Promoted Mesoporous Manganese Oxide

Sourav Biswas,[†] Biswanath Dutta,[†] Kankana Mullick,[†] Chung-Hao Kuo,[†] Altug S. Poyraz,[†] and Steven L. Suib*,[†,‡]

[†]Department of Chemistry, [‡]Institute of Materials Science, University of Connecticut, U-3060, 55 North Eagleville Road, Storrs, Connecticut 06269 United States

S *Supporting Information*

ABSTRACT: Selective oxidation of amines to imines is one of the most studied reactions in the field of heterogeneous catalysis. Cs ion-promoted mesoporous manganese oxide (meso Cs/MnO$_x$) was synthesized using an inverse surfactant micelle as a soft template. The chemical and structural properties of the mesoporous manganese oxide material were characterized by powder X-ray diffraction, nitrogen sorption, electron microscopy, and X-ray photoelectron spectra. The meso-Cs/MnO$_x$ material presented an aggregated nanocrystalline nature with monomodal mesoporous size distributions. The catalyst was found to be effective in the oxidation of amines to imines under aerobic conditions. The meso Cs/MnO$_x$ exhibited oxidation of primary, secondary, cyclic, aromatic, and aliphatic amines to imines, and the conversions reached as high as >99%. The catalyst was also effective in oxidative cross-condensation of two different amines to produce asymmetrically substituted imines. Surface-active Mn^{3+} species along with labile lattice oxygen were found to play an important role in the catalytic activity. Mild reaction conditions (air atmosphere and absence of any oxidative or basic promoters), ease of product separation by simple filtration, and significant reusability make this mesoporous manganese oxide material an economical and ecofriendly catalyst for the syntheses of versatile imine derivatives.

KEYWORDS: *amine oxidation, mesoporous material, manganese oxide, ion-promoted, heterogeneous catalysis*
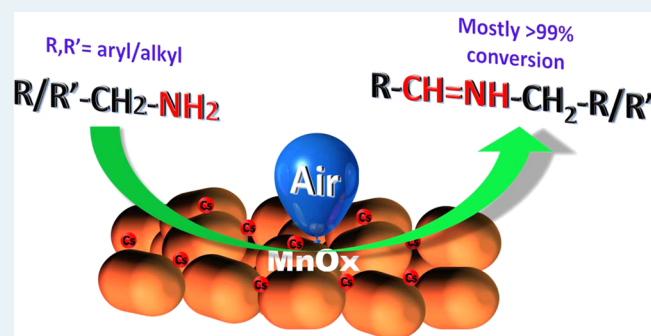
1. INTRODUCTION

Imines are a class of nitrogen-based compounds with high reactivity due to the presence of unsaturated C=N double bonds. Derivatives of imines have versatile uses in the production of heterocyclic chemicals and pharmaceutical compounds.[1] The traditional approach of imine synthesis involves a condensation reaction between amines and carbonyl compounds. The process requires Lewis acid catalysts, dehydrating agents, activated aldehydes, and prolonged reaction time, therefore restraining the use of this process practically and environmentally.[2,3] As an alternative approach, the direct oxidation of amines has attracted considerable attention for synthesis of imines. Stoichiometric oxidants such as chromate, permanganate, and 2-iodoxybenzoic acid[4] have been used for the oxidation of amines to imines. However, the use of stoichiometric oxidants has several drawbacks, which are the production of undesirable toxic waste and difficulties in product separation.

Improvement of the catalytic oxidation reaction is a captivating and demanding technology in the field of heterogeneous catalysis. Because of considerable increasing environmental concerns, chemists are constantly looking for cleaner synthetic strategies with high atom economy. In comparison with different kinds of oxidizing agents, air is the most economical and green oxidant. Catalytic oxidation under ambient aerobic conditions has been recognized as the ultimate reaction in past decades in the production of fine chemicals.[5,6] Some established catalytic systems for the oxidation of amines to imines include precious-metal-based catalysts, such as palladium, platinum, and gold;[7−12] other systems, such as ruthenium,[13,14] graphene oxide,[15] metal organic frameworks,[16] α-MnO$_2$,[17] and copper;[18−21] and photocatalysts, such as TiO$_2$,[22,23] BiVO$_4$,[24] and Nb$_2$O$_5$.[25] Despite good yields and selectivity, all of the catalysts either have cumbersome preparation methods or require the use of harsh reaction conditions, such as high pressure, light irradiation, and use of oxidative promoters.[20,26] Moreover, limited activity of aliphatic amines with undesired side reactions is another flaw for the reported systems.[27,28] Despite good activity in the syntheses of symmetrical imines, syntheses of asymmetrically substituted imines by cross-condensation of two amines have barely been discussed.[29,30] Therefore, design of an effective heterogeneous catalyst system for the oxidation of amines is desirable and ideally involves mild aerobic atmospheric conditions, high

TOF, avoidance of any additives, and high reusability and activity toward syntheses of symmetrical and asymmetrical substituted imines.

Mesoporous metal oxides are capable of acting as superior heterogeneous catalysts because of their intrinsic features of high surface area and tunable pore sizes.[31−33] A high surface area provides a higher concentration of active sites per unit mass of substrate, whereas a tunable pore size expedites adsorption and mass transfer. Among the various metal oxides, manganese oxides acquired a great deal of interest in catalytic oxidation reactions. The catalytic properties of manganese oxide are strongly related to the exchangeable redox properties of different oxidation states of Mn.[34] The concepts of structural defects, lattice oxygen, and acid−base properties are fundamental for understanding the origin of catalytic performance of manganese oxide. We have previously demonstrated that surface-residing promoter ions can enhance the catalytic activity of manganese oxides.[35−37] A new series of mesoporous materials [University of Connecticut (UCT) mesoporous materials] has been discovered recently by our group.[38] Unlike conventional mesoporous material synthesis, an inverse surfactant micelle was used as a soft template. Precise control over the pore size, surface area, and crystallinity by simple heat treatment cycles make these types of materials superior to their nonporous counterparts in different catalytic applications, such as oxidation of alcohols, low-temperature CO and CH_4 oxidation, and water-splitting reactions.[37,39−42]

With the UCT material synthesis approach, we have recently reported mesoporous Cs-promoted manganese oxide as an efficient oxidation catalyst.[37] Incorporation of a trace amount of Cs in the manganese oxide resulted in superior activity enhancement in the aerobic oxidation reactions. For instance, the catalyst was found to oxidize structurally different alcohols to aldehydes selectively (100% selectivity) with very high conversion (as high as 100%). The oxidation ability was further confirmed by the activation of relatively inert C−H bonds under solvent-free conditions. The presence of surface-active Mn^{3+} species along with accessible lattice oxygen and the bifunctional character (oxidative and basic) of the catalyst were found to be the factors responsible for the catalytic performance. Herein, we report the aerobic oxidation of amines to imines and oxidative cross-condensation of two different amines (benzylamine and other aromatic and aliphatic amines) with mesoporous Cs-promoted manganese oxide material (meso Cs/MnO_x). Use of air as the sole oxidant, ambient reaction conditions, high yields of imines, and absence of additives make this process superior to other heterogeneous catalytic systems. The mechanistic pathways and kinetic analysis were also studied in detail. This is the first example of an additive-free and nonphotochemical heterogeneous catalytic system for synthesizing symmetrical and asymmetrical imines from diverse amines under aerobic atmospheric conditions.

2. EXPERIMENTAL SECTION

2.1. Synthesis of Mesoporous Cs/MnO$_x$.
In a typical synthesis, 0.02 mol of manganese nitrate tetrahydrate (Mn-$(NO_3)_2 \cdot 4H_2O$) and 0.134 mol of 1-butanol were added into a 120 mL beaker. To this solution, 0.00034 mol of poly(ethylene glycol)-*block*-poly(propylene glycol)-*block*-poly(ethylene glycol) (Pluronic P123, $PEO_{20}PPO_{70}PEO_{20}$, molar mass 5750 g mol^{-1}) and 0.032 mol of concentrated nitric acid (HNO_3) were added and stirred at room temperature until the solution

became clear (light pink). To this clear solution, 200 μL of 1.0 M cesium nitrate ($CsNO_3$) aqueous solution was added, maintaining the Mn/Cs molar ratio of 100/1. The resulting clear solution was then kept in an oven at 120 °C for 3 h under air. The black product was collected and washed with excess ethanol, centrifuged, and dried in a vacuum oven overnight. At the end, the dried black powders were subjected to a heating cycle. First, they were heated at 150 °C for 12 h and cooled to room temperature under ambient conditions, followed by a second heating step of 250 °C for 3 h. Mesoporous MnO_x was synthesized by the same procedure without adding any $CsNO_3$ solution.

2.2. Catalyst Characterization.
Powder X-ray diffraction (PXRD) measurements were performed on a Rigaku Ultima IV diffractometer (Cu Kα radiation, λ = 1.5406 Å) with an operating voltage of 40 kV and a current of 44 mA. The low-angle PXRD pattern was collected over a 2θ range of 0.5−8° with a continuous scan rate of 0.5° min^{-1}, where the wide-angle PXRD pattern was collected over a 2θ range of 5−75° with a continuous scan rate of 2.0° min^{-1}. Nitrogen sorption experiments were performed by a Quantachrome Autosorb-1-1C automated adsorption system. The material was degassed at 150 °C for 5 h (ramp rate 10 °C/min) under helium prior to measurement. The surface area was calculated using the Brunauer−Emmett−Teller (BET) method, and the Barrett−Joyner−Halenda (BJH) method was utilized to calculate the pore sizes and pore volume from the desorption branch of the isotherm. The surface morphology was determined with a Zeiss DSM 982 Gemini field emission scanning electron microscope (FE-SEM) with a Schottky emitter at an accelerating voltage of 2.0 kV having a beam current of 1.0 mA.

High-resolution transmission electron microscopy (HR-TEM) experiments were carried out on a JEOL 2010 FasTEM microscope at an operating voltage of 200 kV. The samples were prepared by casting the suspension of material onto a carbon-coated copper grid. X-ray photoelectron spectroscopy (XPS) was done on a PHI model 590 spectrometer with multiprobes (ΦPhysical Electronics Industries Inc.), using Al K radiation (λ = 1486.6 eV) as the radiation source and was fitted using CasaXPS software (version 2.3.12). The powder samples were pressed onto carbon tape mounted on adhesive copper tape stuck to a sample stage placed in the analysis chamber. For correction of surface charging, the C 1s photoelectron line at 284.6 eV was taken as a reference. A mixture of Gaussian (70%) and Lorentzian (30%) functions was used for the least-squares curve-fitting procedure. The temperature-programmed desorption (TPD) experiments were performed with a Thermolyne 79300 model tube furnace equipped with an MKS gas analyzer coupled with a quadrupole mass selective detector. The samples were treated with Ar for 2 h at 250 °C before the experiment. Ar was used as a carrier gas in the experiments at a constant flow rate in the temperature range 50−600 °C at a ramp of 10 °C min^{-1}. The amount of Cs in the material was determined with a PerkinElmer/DRC-e inductively coupled plasma mass spectrometer (ICP-MS) CETAC laser ablation unit, whereas a PerkinElmer Optima 7300DV inductively coupled plasma optical emission spectrometer (ICP-OES) was used to determine the Mn concentration.

2.3. Catalytic Activity Measurements.
2.3.1. Oxidation of Amines to Imines. In a typical amine oxidation reaction, a mixture of amine (0.5 mmol), catalyst (25 mg), and toluene (5 mL) was added in a 25 mL round-bottom flask equipped with a condenser. The reaction mixture was heated to reflux under
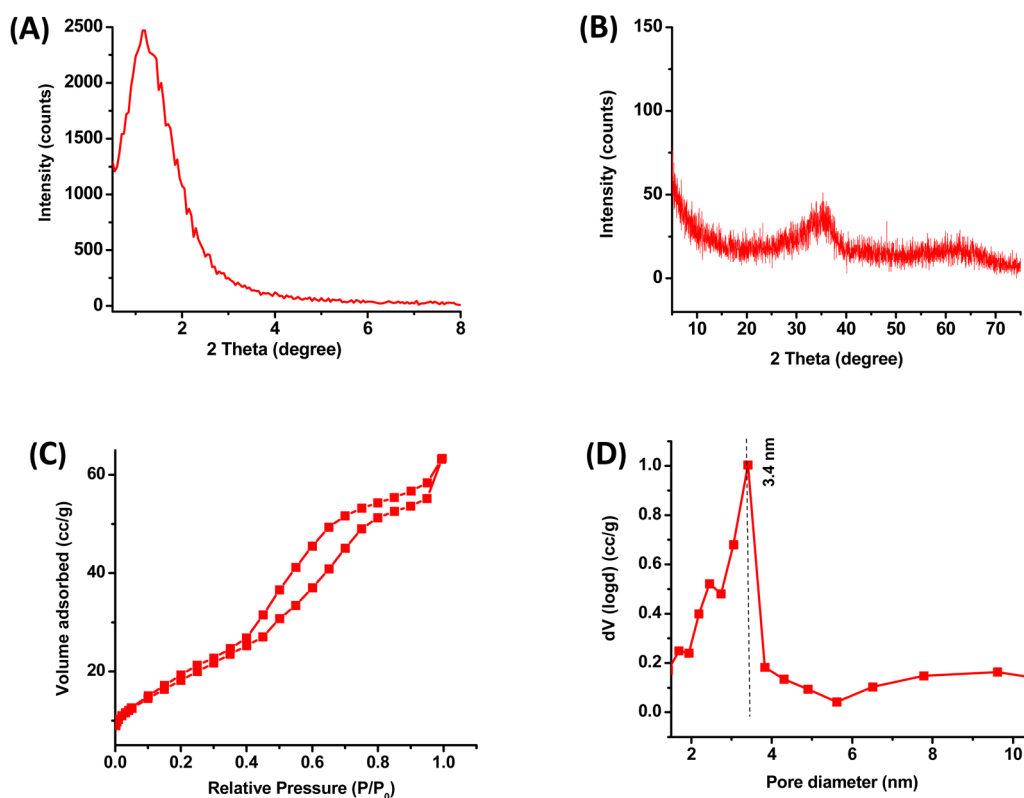
Figure 1. Structural characterization of meso Cs/MnO$_x$. PXRD patterns: (A) low angle (0.5° −8°), (B) wide angle (5°−75°), (C) N$_2$ sorption isotherm, and (D) BJH desorption pore size distribution.
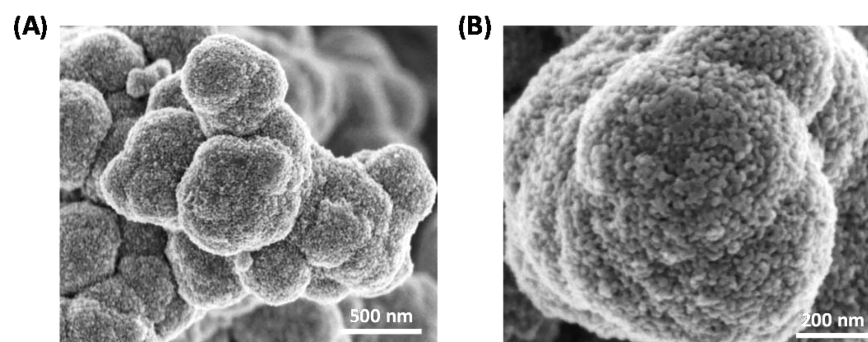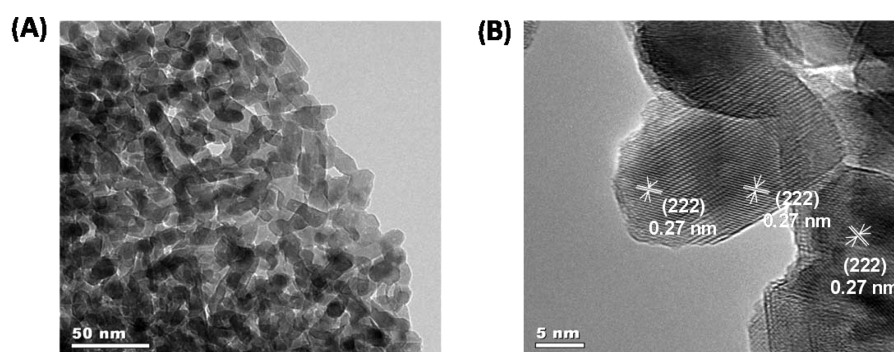

Figure 2. SEM images of meso Cs/MnO$_x$ at (A) low and (B) higher magnifications.

vigorous stirring (700 rpm) for the required time under an air balloon. After reaction, the mixture was cooled, and the catalyst was removed by filtration. The product analysis was done using GC/MS (gas chromatography/mass spectrometry). The conversion was determined on the basis of the concentration of the amines. The selectivity was calculated on the basis of imines, aldehydes, and cyanides as the only products. Most reactions were repeated twice, and the average values were used.

Pure imines were obtained by washing and evaporation of the solvent. The reaction was cooled to room temperature after completion (having a negligible amount of aldehydes and cyanides along with imines). The catalyst was removed by centrifugation and washed several times with toluene. The filtrate was collected and kept for evaporation of solvent and finally dried under vacuum. The imine products were identified by the ^{1}H NMR and ^{13}C NMR spectra.

2.3.2. Cross-Coupling of Amines. In a typical cross-coupling reaction, a mixture (1/3 molar ratio) of benzylamine and other aliphatic and aromatic amines, catalyst (25 mg), and toluene (5 mL) were put in a 25 mL round-bottom flask equipped with a condenser. The reaction mixture was heated to reflux with vigorous stirring (700 rpm) for the required time under an air balloon. After reaction, the mixture was cooled, the catalyst was removed by filtration, and GC/MS was used to analyze the filtrate. The conversion was determined based on concentration of benzylamine (limiting reactant). The selectivity was calculated on the basis of the self- and cross-products of benzylamine.

2.4. Analysis of Reaction Products. The GC/MS analyses were performed by a 7820A GC system connected to a mass detector of 5975 series MSD from Agilent Technologies and a nonpolar cross-linked methyl siloxane column with dimensions of 12 in ×0.200 mm × 0.33 μm was used. The ^{1}H and ^{13}C NMR spectra were recorded on a Bruker

Figure 3. TEM images of meso Cs/MnO$_x$ at (A) low and (B) higher magnification. The measured lattice distances of 0.27 nm can be indexed to bixbyite Mn$_2$O$_3$ (222) planes.

Table 1. Optimization of Oxidative Coupling of 4-Methoxy Benzyl Amine[a]

entry	solvent	temp (°C)	time (h)	oxidant	conversion[b] (%)	selectivity[c] (%)	TON[d]
1	methanol	60	8	air	50	94	0.84
2	dioxane	100	8	air	55	100	0.92
3	hexane	66	8	air	44	100	0.73
4	toluene	110	8	air	100	80	1.67
5	toluene	80	8	air	45	100	0.75
6[e]	toluene	110	8	air	100	85	0.83
7[f]	toluene	110	5	air	100	96	3.33
8[f]	toluene	110	3	O$_2$	90	100	3.00
9[f]	toluene	110	8	N$_2$	53	100	1.76

[a]Reaction conditions: 4-methoxy benzyl amine (0.5 mmol), meso Cs/MnO$_x$ (50 mg), solvent (5 mL), air balloon, 3−5 h. [b]Conversions were determined by GC/MS on the basis of the concentration of amines. [c]The other products were aldehyde and cyanide. [d]TON = moles of amine converted per mole of catalyst. [e]100 mg of catalyst. [f]25 mg of catalyst.

AVANCE III- 400 MHz spectrometer. ^{1}H NMR spectra were collected at 400 MHz with chemical shift referenced to the residual peak in CDCl$_3$ (δ: H 7.26 ppm). ^{13}C NMR spectra were collected at 100 MHz and referenced to the residual peak in CDCl$_3$ (δ: C 77.0 ppm). Multiplicities are written as s (singlet), d (doublet), t (triplet), and m (multiplet).
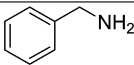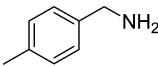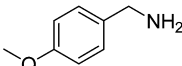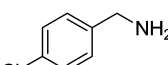
3. RESULTS
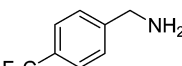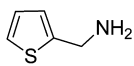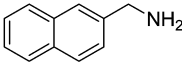
3.1. Structural characterization of Meso Cs/MnO$_x$. The physicochemical and morphological features of the material were characterized extensively by powder X-ray diffraction (PXRD), N$_2$ sorption, scanning electron microscopy (SEM), transmission electron microscopy (TEM), X-ray photoelectron spectroscopy (XPS), temperature-programmed desorption (TPD) and inductive coupled plasma (ICP) techniques. The PXRD pattern (Figure 1A) at low angle region (0.5−8°) displayed a single peak, which represented the irregular porous nature of the materials. No distinct diffraction pattern was observed in the wide angle (5−75°) range (Figure 1B), which indicated the poorly crystalline nature of the material. The mesoporosity of the material was confirmed by N$_2$ sorption exper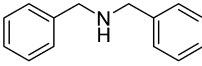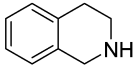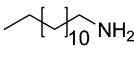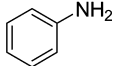iments (Figure 1C), where a type IV adsorption isotherm followed by a type I hysteresis loop was observed. Pore size of meso Cs/MnOx was calculated as 3.4 nm by the BJH method (Figure 1D) from the desorption branch of the isotherm, whereas the surface area was (calculated by BET method) 79 m^2 g^{-1}. SEM images (Figure 2) showed that aggregated nanoparticles formed quasi-spherical micrometer-sized mor-

phology. The TEM image (Figure 3A) also revealed the random packing of nano-oxide particles. Unlike PXRD, the high resolution TEM (Figure 3B) indicated the crystalline nature of the material. The lattice fringes were calculated as 0.27 nm, which can be correlated to the (222) plane of Mn$_2$O$_3$ (bixbyite) phase, which was in agreement with the literature findings.[37] Poorly crystalline nature of the material can be the reason for absence of any diffraction peaks under PXRD.

The Mn 2p XPS spectra in Figure S1B consist of two peaks, which were assigned as Mn 2p$_{3/2}$ and Mn 2p$_{1/2}$ core levels. The binding energy of 641.5 and 653.5 eV can be attributed to the Mn^{3+} oxidation state.[37,43] The O 1S spectra (Figure S1A) showed a broad peak of binding energy in the range of ∼527 to 536 eV, indicating the presence of multiple oxygen species. Deconvolution of O 1s spectra (Figure S1A) specified the existence of three different binding oxygen species: namely, structural or lattice oxygen (O$_s$), surface adsorbed oxygen (O$_{ads}$), and adsorbed water or hydroxyl group (O$_{mw}$).[43] The relative amount of structural oxygen (O$_s$) was higher than the other type of oxygen species (Figure S1, Table S1).

O$_2$-TPD data under a stream of Ar gas are shown in Figure S2. In general, desorptions of surface-adsorbed oxygen species and labile lattice oxygen species with different Mn−O bond strengths cause the appearance of peaks in the O$_2$-TPD profile. A major loss of O$_2$ from the meso Cs/MnO$_x$ material, which can be ascribed as the evolution of lattice oxygen from the manganese oxide[44] (Figure S2), was observed at 570 °C. ICP-MS was employed to verify the amount of Cs in the material. A

Table 2. Aerobic Oxidation of Amines to Imines by Meso Cs/MnO$_x$[a]

Entry	Substrate	Time (h)	Conversion[b] (%)	Selectivity[b] (%)	TON[c]
1		3	>99(82)	93	3.33
2		4	>99	75	3.33
3		5	>99(80)	96	3.33
4		2	>99	98	3.33
5		2	>99(96)	96	3.33
6		4	>99	92	3.33
7		4	>99	80	3.33
8[d]		20	45	99	1.50
9[d]		3	>99	95	3.33
10		24	>99	50	3.33
11[e]		4	15	nd	nd

[a]Reaction conditions: amines (0.5 mmol), meso Cs/MnO$_x$ (25 mg), toluene (5 mL), 110 °C, air balloon. [b]Conversion and selectivity was determined by GC/MS on the basis of the concentration of the amines. Numbers in parentheses refer to yields of isolated products. [c]TON = moles of amines converted/mol of catalyst. [d]Meso Cs/MnO$_x$ (50 mg). [e]Azobenzene was the only product; nd = not detected.

very low concentration of Cs (Mn/Cs molar ratio was 604/1), quite different from the nominal ratio (100/1), was detected. Excess ions were probably removed by washing.

3.2. Optimization of Reaction Condition. Oxidative coupling of amines to imines over the metal oxides has been discussed extensively in the literature,[15,17] and a generally accepted reaction mechanism is described in Scheme S1. The reaction is initiated by the oxidative dehydrogenation of amines to form the RCH=NH intermediate, followed by reacting with the water molecules to form aldehyde with exclusion of ammonia. The intermediate aldehyde was then condensed with the amines to form the target imine molecules.

At the beginning of our studies, we selected the oxidation of 4-methoxybenzylamine as a model reaction for developing the optimal reaction conditions. First, the reactions were performed by meso Cs/MnO$_x$ in solvents of different polarities at their respective boiling point temperatures (entries 1−4, Table 1). Toluene (the one with highest boiling point, 110 °C) gave the highest conversion (>99%) (entry 4, Table 1) and selectivity of 80% toward the imine among the tested solvents and was

selected for the testing. Further optimization was employed to increase the selectivity of the imine formation over cyanide and aldehyde intermediates. Because the formations of other side products are favored at high temperatures, the reaction was performed at relatively lower temperature (80 °C). A high selectivity of imine (>99%) can be achieved at 80 °C, but conversion decreased significantly to 45% (entry 5, Table 1). Furthermore, the variation of the selectivity for imine with catalyst loading was established for meso Cs/MnO$_x$ (entries 5−7, Table 1). Although no significant changes in conversion and selectivity were observed with the catalyst loading of 100 mg (entry 6, Table 1), decreasing the catalyst amount to 25 mg was found to be sufficient to drive the reaction toward a quantitative conversion (>99%) and high selectivity (96%) (entry 7, Table 1). The reaction was completed in 5 h in aerobic atmospheric conditions without use of any additives. When pure oxygen was used instead of air as oxidant (entry 8, Table 1), the reaction was completed at even shorter times (as short as 3 h). A significant decrease in the conversion (53%) was observed under nitrogen atmosphere in 8 h (entry 9, Table 1).

3.3. Comparison with Different Catalysts. Comparison with the well-established redox catalysts is essential for newly developed highly active catalysts. Very low conversion (10%) was achieved in the absence of any catalyst in 8 h (entry 7, Table S2). No improvement in the conversion was observed using a commercial nonporous Mn_2O_3, indicating it was totally inactive in the present condition (entry 6, Table S2). Using potassium-containing manganese oxide octahedral molecular sieves (K-OMS-2[45]), the selectivity for imines decreased drastically, to 42% with the formation of a high concentration of cyanide (due to dehydrogenation of amine) and aldehyde products. Other manganese oxide-based catalysts, such as amorphous manganese oxide and birnessite, were also tested under the present reaction conditions (entries 4−5, Table S2). Meso MnO_x without Cs promoter (synthesized by the same UCT method) resulted in a similar (>99%) conversion (entry 2, Table S2) but much lower selectivity (78%) compared with meso Cs/MnO_x (96% selectivity).

To determine the role of Cs in the present amine oxidation catalytic system, a series of experiments were performed by changing the Cs loading in the material. The aerobic oxidation of a relatively inert secondary amine (1,2,3,4-tetrahydroisoquinoline) was selected as the model reaction. A remarkable increase in the conversion (Table S3) was observed when Cs was incorporated in the meso MnO_x material. The non-promoted meso MnO_x material exhibited only 12% conversion (entry 1, Table S3) after 1 h, whereas 87−95% conversions (entries 2−4, Table S3) were achieved by Cs incorporation. The meso Cs/MnO_x material with the highest Cs loading (0.16%) gave the maximum conversion (94%) under identical reaction conditions (entry 4, Table S3).

All of these factors (high activity for both primary and secondary amines, air as oxidant and atmospheric condition) allowed meso Cs/MnO_x preferably to be superior to the other reported catalytic systems in which a high pressure oxygen set-up (graphene oxide), *tert*-butyl hydroperoxide (TBHP) additives (α-MnO_2), light irradiation (photocatalysts), or precious-metal-based systems were inevitable for achieving the catalytic efficiency.

3.4. Oxidation of Amines to Imines. Having analyzed the optimum reaction conditions for 4-methoxybenzylamine oxidation, the substrate scope and limitations were explored for different types of amines. The results of catalytic oxidation of various amines, including aromatic, aliphatic, primary and secondary amine derivatives, are listed in Table 2. The isolated yield of some of the imines are given in Table 2 (see values in parentheses), along with their ^1H NMR and ^{13}C NMR data (see the Supporting Information). Meso Cs/MnO_x was able to oxidize aromatic (entries 1−9, Table 2), aliphatic (entry 10, Table 2), primary (entries 1−7, Table 2), secondary (entries 8−9, Table 2), and cyclic (entry 9, Table 2) amines to the corresponding imines with excellent conversion and selectivity. No dehalogenated product was detected in the case of the amines with halogen substitution (entries 4−5, Table 2). Amine containing S as heteroatom was converted to the imine effectively (entry 6, Table 2).

The catalyst was also useful for oxidation of the relatively bulky biphenyl (1-naphthylmethylamine) system (entry 7, Table 2). In the case of oxidation of the secondary amine (entry 8, Table 2), conversion was less, and a much longer reaction time (20 h) and as well as higher amount of catalyst (50 mg) were required. Oxidation of 1,2,3,4-tetrahydroisoquinoline (entry 9, Table 2) produced a cyclic imine with notable

conversion (95%) and selectivity (95%). Remarkable catalytic activity of meso Cs/MnO_x was attributed to the successful oxidation of a long-chain inactive aliphatic amine (1-dodecylamine) toward the corresponding imines (entry 10, Table 2), although a longer reaction time (24 h) was required and the selectivity was much smaller (50%). The other byproduct was dodecanenitrile, which was formed by the dehydrogenation of the reactive RCH=NH intermediate. On the other hand, oxidation of aniline (lacking of α-H atoms) produced azo benzene as the only oxidation product (entry 11, Table 2).

The oxidation of benzylamine derivatives bearing electron-donating (entries 2−3, Table 2) as well as electron-withdrawing groups (entries 4−5, Table 2) were successfully converted to the imines. Benzylamine with electron-withdrawing groups (CF_3 and Cl) displayed >99% conversion with a TOF of 1.56 h^{-1}, whereas the presence of electron-donating groups (OCH_3 and CH_3) resulted in >99% conversion but a lower TOF (0.78 h^{-1} for 4-methylbenzylamine and 0.68 h^{-1} for 4-methoxybenzylamine). The Hammett equation can be used to interpret the electronic or steric influence of the substituents on the reaction rate.[46] The relative rates of oxidation of para-substituted benzylamines (p-Cl, p-H, p-Me, p-OMe) were investigated. A linear relationship was found between $\ln(k_x/k_H)$ and the Brown−Okamato constant (σ_p^+) (Figure 4). The slope
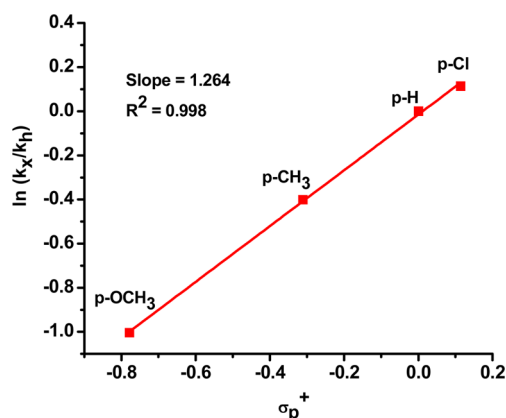
Figure 4. Hammett plot of competitive oxidation of para-substituted benzylamine at 15 min of reaction time. Reaction conditions: amine (0.5 mmol), catalyst (25 mg), solvent (5 mL), 110 °C, air balloon, 15 min. A linear relationship between $\ln(k_x/k_H)$ and the Brown−Okamoto constant (σ_p^+) for para-substituted benzylamines with a slope (ρ) of 1.264 were obtained, which indicated the formation of a negatively charged intermediate.

of the plot resulted a reaction constant (ρ) value of 1.264, which illustrated the development of a negative charge at the reaction center in the transition state of the rate-limiting step.[47]

3.5. Cross Coupling of Amines. Excellent activities in the Cs/MnO_x-mediated oxidation of amines to imines encouraged us to check the feasibility of this atmospheric aerobic protocol in the synthesis of unsymmetrical imines. Reactions between benzylamine and 4-methoxybenzylamine were performed at different molar ratios (entries 1−3, Table 3). The reaction having 1/3 molar ratio of benzylamine/4-methoxybenzylamine exhibited the highest selectivity toward the unsymmetrical imine (77% selectivity), with minimum formation of symmetrical imine (23% selectivity), then a variety of structurally different amines and benzylamine were tested with the best optimized reaction condition (1/3 molar ratio). Using amines with electron-releasing and electron-withdrawing groups

Table 3. Aerobic Oxidative Cross Coupling of Benzylamine with Different Amines[a]

Entry	Substrate	Molar ratio[b]	Conversion[c] (%)	Selectivity[d] (%)	
				1a	**2a**
1	4-methoxybenzylamine	2/1	>99	62	25
2	4-methoxybenzylamine	1/2	>99	30	70
3	4-methoxybenzylamine	1/3	>99	23	77
4	4-methylbenzylamine	1/3	>99	10	89
5	4-(trifluoromethyl)benzylamine	1/3	>99	27	73
6	thiophene-2-methylamine	1/3	>99	42	58
7	butylamine	1/3	>99	nd	>99
8	dodecylamine	1/3	>99	nd	>99
9	aniline	1/3	15	70	30

[a]Reaction conditions: benzylamine and other aromatic and aliphatic amines (0.5 mmol), meso Cs/MnO$_x$ (25 mg), toluene (5 mL), 110 °C, 3 h, air balloon. [b]Molar ratio of benzylamine and different amines. [c]Conversion was determined by GC/MS on the basis of the concentration of benzylamine. [d]Selectivity was calculated on the basis of the self-coupled (1a) and cross-coupled (2a) products of benzylamine; nd = not detected.

produced unsymmetrical imines with high (73–89%) selectivity (entries 3–5, Table 3). An unsymmetrical imine having a heteroatom S was synthesized (58% selectivity) by the reaction between benzylamine and 2-thiopheneamine using the established method (entry 6, Table 3). The method was further utilized to perform a reaction between an aromatic amine (benzylamine) and aliphatic amines (butylamine and dodecylamine) (entries 7–8, Table 3). The selectivity (>99%) toward the unsymmetrical imines was excellent compared with the coupling of two aromatic amines. A very low selectivity (30% selectivity) of unsymmetrical imine was observed by a reaction between benzylamine and aniline.

3.6. Reusability and Heterogeneity. Steady reusability and negligible leaching of active species are the two important aspects of the heterogeneous catalysts. The reusability test was conducted for the oxidation of 4-methoxybenzylamine. At the end of the reaction, the catalyst was removed by filtration, washed with ethanol, and reactivated at 250 °C for 45 min prior to reuse. Reactivation was required to remove the adsorbed species from the catalyst surface. The catalyst retained the activity and selectivity even after the fourth cycle (Figure S3A). PXRD analyses of as-synthesized and the recovered catalysts

indicated that the amorphous nature of the catalyst was preserved (Figure S3B). The hot filtration test was also carried out to verify any possible leaching of active species from the catalyst surface. No further consumption of 4-methoxybenzylamine took place after filtering off the catalyst at 47% conversion (Figure S4). Moreover, a very minute change in the Cs amount (0.04%) was observed in the meso Cs/MnO$_x$ after the reaction by ICP-MS. All of these results signified the truly heterogeneous nature of meso Cs/MnO$_x$, which not only was active but also had sustainability and recyclability.

3.7. Kinetic and Mechanistic Study. The high activity and selectivity of meso Cs/MnO$_x$ as an amine oxidation catalyst system motivated us to gain an insight into the mechanistic details of the reaction. To determine if any radical intermediates were involved in the reaction, we used a radical scavenger (2,6-di-*tert*-butyl-4-methylphenol). The scavenger had no effect on the reaction rate of 4-methoxybenzylamine oxidation, which ruled out the formation of any radical intermediates. Time-dependent experiments on the oxidation of 4-methoxybenzylamine were conducted using meso Cs/MnO$_x$ to study the reaction kinetics (Figure S5). Continuous sampling was undertaken in the course of 1 h, and conversion

and selectivity were determined by GC/MS. Formation of benzaldehyde in minutes was observed during the reaction pathway, along with the desired imine as the major product. Kinetic experiments depicted a first-order rate equation with respect to the amine (Figure S6) having a rate constant of 0.42 min^{-1}. The apparent activation energy was calculated as 11.5 kJ mol^{-1} from the Arrhenius plot (Figure S7). Kinetically relevant elementary steps in the reaction pathways were measured by changing the benzylic H to D in benzylamine. From the first-order reaction plot between ln[benzylamine] and ln-[benzylamine-α,α-d$_2$], the obtained kinetic isotope effect (KIE) value was 2.04 (Figure S8). This result signified abstraction of the α C−H proton of amine as the rate-determining step in the reaction.

4. DISCUSSIONS

The material was synthesized following the synthesis procedure of University of Connecticut (UCT) mesoporous materials.[38] Transition metal and ion precursors loaded with inverse micelles grew packed in a random fashion to build the mesoporous structure. The reaction solvent was acidic (HNO$_3$) 1-butanol solution. Evaporation of the solvent (by heat treatment) along with the NO$_x$ formation (by thermal decomposition of nitrates) had driven the reaction. The nitrate ions had dual roles. First, the hydrotropic[48] nature of the nitrate ions hydrated the core of the inverse surfactant micelles by penetrating through it, which pulled the positively charged manganese oxo-clusters to the core of the inverse micelles by increasing the solubility. Second, the nitrate ions decomposed to form the NO$_x$ species, which controlled the pH and the sol gel chemistry of the Mn sols. Solvent extraction by ethanol was performed to remove surfactants from the mesoporous materials. Chemisorbed species (nitrates and carboxylates) were removed by a heat treatment at 150 °C for 12 h and were followed by a second heat treatment at 250 °C for 3 h.

Catalytic aerobic oxidation of amines to imines was performed by meso Cs/MnO$_x$. Diverse amine derivatives were converted to the corresponding imines efficiently. Catalytic reaction of halobenzene derivatives without dehalogenation is a challenge.[49] We tested oxidation of 4-chlorobenzylamine to verify any dehalogenation. A >99% selectivity toward imine with no dehalogenated products was observed (entries 4−5, Table 2), indicating the effectiveness of meso Cs/MnO$_x$ in the oxidation of halogen-containing substrates. Substrates bearing hetero atoms such as S or N are known to poison transition metal oxide-based catalysts because of the strong coordination of the heteroatom to the transition metal centers.[50] However, in the present study, 2-thiophene benzylamine was converted efficiently to the corresponding imines with no significant change of TOF and selectivity compared with the benzylamines (entry 6, Table 2).

The oxidation ability of meso Cs/MnO$_x$ was further tested for selective oxidation of relatively inert secondary amines (entries 8−9, Table 2). As observed, the secondary amines can also be transformed to the corresponding imines with very high conversions (45−95%) and excellent selectivity (95−99%), but a much longer reaction time (20 h) and a higher amount of catalysts (50 mg) were required. This may be due to the steric effect because it was relatively difficult to abstract the H atoms next to the N−H group. The reaction with dibenzylamine produced benzaldehyde as the side product, which can be attributed to the oxidative cleavage of C═N bond of imine. Aliphatic amines are relatively difficult to oxidize, as mentioned

in the previous studies;[51] however, in case of the oxidation of a long-chain, inactive 1-dodecylamine by meso Cs/MnO$_x$, an imine was formed having 24 carbon atoms. Such a reaction with an inactive aliphatic amines has not been observed in previous studies. The bifunctional nature (oxidative and basic) of the meso Cs/MnO$_x$ is believed to be the reason for the superior activity of the long-chain 1-dodecylamine because the dehydrogenation of amine can be promoted by the basic nature of the catalyst.[52] The easy diffusion and transportation of 1-dodecylamine in the mesoporous network may be the other reason behind the activity. The lower selectivity (50%) of the product imine compared with the aromatic systems (mostly >90%) can be attributed to the lower stabilization due to the absence of conjugated aromatic rings.

Along with symmetrical imine formation, the catalyst was also effective for the formation of asymmetrical imines. Depending on the molar ratio and the nucleophilic properties of the partner amines, asymmetrical imines can be synthesized efficiently. The reaction between an aromatic amine (benzylamine) and aliphatic amines (1-butylamine and 1-dodecylamine) produced asymmetrical imine with >99% selectivity. This can be attributed to the higher nucleophilic nature of aliphatic amines than that of aromatic amines. Once the benzaldehyde was formed, the more nucleophilic aliphatic amines competed with the benzylamine to minimize the self-coupling and yielded the unsymmetrical amines with a very high selectivity (>99%). The difference in the nucleophilic properties also explained the relatively less selective unsymmetrical imine production from benzylamine and aniline (entry 9, Table 3). The lower nucleophilic property of the anilines than the benzylamine drove the reaction toward self-oxidative coupling of the benzylamines (70% selectivity).

In general, a Mars-Van-Krevelen mechanism,[53] is anticipated to occur for oxidation types of reactions over manganese oxides. According to the mechanism, structural defects and labile lattice oxygen are the key properties of manganese oxide catalysts. In this study, the poorly crystalline nature of the meso Cs/MnO$_x$ promoted a facile supply of lattice oxygen, as observed by XPS and O$_2$-TPD studies. The basicities of the metal oxides are known to be increased as a result of the presence of electropositive alkali metal ions. In this study, incorporation of trace amounts of electropositive Cs ions induced basicity in the meso MnO$_x$, which can be considered surface defects of the material.[54,55] As shown in CO$_2$ chemisorption experiments (Figure S9), an increase in the CO$_2$ uptake was observed for the meso Cs/MnO$_x$ material at three different temperatures, which indicated an increase in the basicity of the meso MnO$_x$ after incorporation of Cs. The presence of basic sites in the meso Cs/MnO$_x$ material can enhance the oxidative dehydrogenation of amine by aiding the deprotonation of an α C−H bond.[52] Secondary amines are considered tough substrates for oxidation because of the inactiveness of α C−H bonds;[24] however, in our study, an 87% increase in the conversion (entries 1−4, Table S3) of the oxidation of an inert secondary amine (1,2,3,4-tetrahydroisoquinoline) was observed by incorporation of Cs into meso MnO$_x$. All of these experiments signified the poorly crystalline and bifunctional nature of meso Cs/MnO$_x$ toward the augmented catalytic activity in oxidation of amines.

On the basis of experiments and the literature, we propose a mechanism for oxidation of amines by meso Cs/MnO$_x$ (Scheme S2). Adsorbed amine molecules transferred an electron to the Mn center, followed by an elimination of an

α C−H proton and an N−H proton to form the RCH=NH intermediate (Scheme S3). The surface-active Mn centers simultaneously involved a one-electron reduction, which can lead to facile release of lattice oxygen and thereby promote the oxidation ability.[56] The labile lattice oxygen reoxidized the Mn center back with production of H_2O_2, which could easily be decomposed over manganese oxide and form water. The abstraction of an α C−H proton produced the negatively charged intermediate (Scheme S3), which was the rate-determining step, as indicated by the linearity of the Hammett plot [positive value (1.264) of reaction constant (ρ)] and isotope labeling study. The trapping of a negatively charged intermediate (by abstraction of α C−H proton) by addition of a radical inhibitor was unsuccessful and may be due to the formation of the intermediate inside the mesoporous network of the catalyst, where transportation of radical inhibitor was not proper. The supply of oxygen from air is crucial for the catalytic activity because loss of lattice oxygen should be replenished by the oxygen from the air. This also was supported by the observation that the elimination of air by nitrogen diminished the reaction rate (entry 9, Table 1). The reactive RCH=NH intermediate was rapidly hydrolyzed by the water and formed the aldehyde, which was condensed with another amine molecule to generate the corresponding imine.

The role of adsorbed water in the catalyst surface (as observed by XPS) is also believed to be significant in the reaction system. A faster reaction rate was observed by the deliberate introduction of water into the reaction, which further confirms our process to follow the above-mentioned reaction pathways.[57] The activation energy (11.5 KJmol^{-1}) was significantly lower than the previous study using α-MnO$_2$ catalyst and TBHP oxidant conducted at room temperature. The activation energy data suggested a lower energy pathway for the meso Cs/MnO$_x$ system at the present reaction conditions. The high surface area and the monomodal uniform mesoporous size distribution are the other important factors related to the catalytic activity. This can be attributed to an enhanced catalytic activity of meso Cs/MnO$_x$ (surface area 78 m^2 g^{-1}) compared with commercial nonporous Mn$_2$O$_3$ (surface area 11 m^2 g^{-1}) The high surface area of meso Cs/MnO$_x$ exposed the lattice oxygen more to the surface, whereas the mesoporous network promoted the adsorption and molecular transportation of the substrates.

5. CONCLUSION

In summary, we have documented mesoporous Cs-promoted manganese oxide as an efficient, selective, and reusable, and therefore environmentally benign catalyst for the catalytic oxidation of amines to imines. The material exhibited uniform monomodal mesoporous size distribution (pore diameter 3.4 nm) with high surface area (78 m^2 g^{-1}). The catalyst was able to oxidize diverse amine derivatives to produce imines with very high percent conversions (as high as >99%) and high selectivity (50−100%). The reactivity of the material toward inactive amines was quite significant. The material was found to be oxidized long-chain aliphatic amines (i.e., 1-dodecylamine) with quantitative conversion (>99%) and high selectivity (50% selectivity). The material was also capable of synthesizing asymmetrical imines by coupling benzylamine and other aromatic and aliphatic amines with excellent selectivity (as high as >99%). Our mechanistic investigation revealed an involvement of surface-active Mn^{3+} species, labile lattice oxygen, and the bifunctional (oxidative and basic) nature of the catalyst toward the augmented catalytic activity. High surface area, low crystalline nanoparticle nature, and presence of mesoporous structure are the other crucial factors. Further investigations of the active sties of the catalyst are underway.

■ ASSOCIATED CONTENT

ⓢ Supporting Information

The Supporting Information is available free of charge on the ACS Publications website at DOI: 10.1021/acscatal.5b00325.

List of chemicals, XPS, O$_2$-TPD, kinetic study, reusability study, isotopic study, calculation of activation energy, and ^{1}H NMR and ^{13}C NMR of typical products (PDF)

■ AUTHOR INFORMATION

Corresponding Author

*Fax: (+1) (860)-486-2981. E-mail: steven.suib@uconn.edu.

Notes

The authors declare no competing financial interest.

■ ACKNOWLEDGMENTS

■ REFERENCES

(1) Kobayashi, S.; Mori, Y.; Fossey, J. S.; Salter, M. M. *Chem. Rev.* **2011**, *111*, 2626−2704.

(2) Naeimi, H.; Salimi, F.; Rabiei, K. . *J. Mol. Catal. A: Chem.* **2006**, *260*, 100−104.

(3) Westheimer, F.; Taguchi, K. *J. Org. Chem.* **1971**, *36*, 1570−1572.

(4) Nicolaou, K.; Mathison, C. J.; Montagnon, T. *Angew. Chem.* **2003**, *115*, 4211−4216.

(5) Zhang, P.; Gong, Y.; Li, H.; Chen, Z.; Wang, Y. *Nat. Commun.* **2013**, *4*, 1593.

(6) Parmeggiani, C.; Cardona, F. *Green Chem.* **2012**, *14*, 547−564.

(7) Wang, J.-R.; Fu, Y.; Zhang, B.-B.; Cui, X.; Liu, L.; Guo, Q.-X. *Tetrahedron Lett.* **2006**, *47*, 8293−8297.

(8) Zhu, B.; Lazar, M.; Trewyn, B. G.; Angelici, R. J. *J. Catal.* **2008**, *260*, 1−6.

(9) Grirrane, A.; Corma, A.; Garcia, H. *J. Catal.* **2009**, *264*, 138−144.

(10) Zhu, B.; Angelici, R. J. *Chem. Commun.* **2007**, 2157−2159.

(11) Yuan, H.; Yoo, W.-J.; Miyamura, H.; Kobayashi, S. *J. Am. Chem. Soc.* **2012**, *134*, 13970−13973.

(12) Yuan, H.; Yoo, W. J.; Miyamura, H.; Kobayashi, S. *Adv. Synth. Catal.* **2012**, *354*, 2899−2904.

(13) Taketoshi, A.; Koizumi, T.-a.; Kanbara, T. *Tetrahedron Lett.* **2010**, *51*, 6457−6459.

(14) Murahashi, S.-I.; Okano, Y.; Sato, H.; Nakae, T.; Komiya, N. *Synlett* **2007**, *2007*, 1675−1678.

(15) Huang, H.; Huang, J.; Liu, Y.-M.; He, H.-Y.; Cao, Y.; Fan, K.-N. *Green Chem.* **2012**, *14*, 930−934.

(16) Dhakshinamoorthy, A.; Alvaro, M.; Garcia, H. *ChemCatChem* **2010**, *2*, 1438−1443.

(17) Zhang, Z.; Wang, F.; Wang, M.; Xu, S.; Chen, H.; Zhang, C.; Xu, J. *Green Chem.* **2014**, *16*, 2523−2527.

(18) Maeda, Y.; Nishimura, T.; Uemura, S. *Bull. Chem. Soc. Jpn.* **2003**, *76*, 2399−2403.

(19) Largeron, M.; Fleury, M.-B. *Science* **2013**, *339*, 43−44.

(20) Hu, Z.; Kerton, F. M. *Org. Biomol. Chem.* **2012**, *10*, 1618−1624.

(21) Sonobe, T.; Oisaki, K.; Kanai, M. *Chem. Sci.* **2012**, *3*, 3249−3255.

(22) Lang, X.; Ji, H.; Chen, C.; Ma, W.; Zhao, J. *Angew. Chem., Int. Ed.* **2011**, *50*, 3934−3937.

(23) Ovoshchnikov, D.; Donoeva, B.; Golovko, V. B. *ACS Catal.* **2015**, *5*, 34−38.

(24) Yuan, B.; Chong, R.; Zhang, B.; Li, J.; Liu, Y.; Li, C. *Chem. Commun.* **2014**, *50*, 15593−15596.

(25) Furukawa, S.; Ohno, Y.; Shishido, T.; Teramura, K.; Tanaka, T. *ACS Catal.* **2011**, *1*, 1150−1153.

(26) Wendlandt, A. E.; Stahl, S. S. *J. Am. Chem. Soc.* **2014**, *136*, 506−512.

(27) Schümperli, M. T.; Hammond, C.; Hermans, I. *ACS Catal.* **2012**, *2*, 1108−1117.

(28) Largeron, M. *Eur. J. Org. Chem.* **2013**, *2013*, 5225−5235.

(29) Largeron, M.; Fleury, M. B. *Angew. Chem., Int. Ed.* **2012**, *51*, 5409−5412.

(30) Wendlandt, A. E.; Stahl, S. S. *Org. Lett.* **2012**, *14*, 2850−2853.

(31) Taguchi, A.; Schüth, F. *Microporous Mesoporous Mater.* **2005**, *77*, 1−45.

(32) Sui, M.; Liu, J.; Sheng, L. *Appl. Catal., B* **2011**, *106*, 195−203.

(33) Perego, C.; Millini, R. *Chem. Soc. Rev.* **2013**, *42*, 3956−3976.

(34) Suib, S. L. *Acc. Chem. Res.* **2008**, *41*, 479−487.

(35) Poyraz, A. S.; Biswas, S.; Genuino, H. C.; Dharmarathna, S.; Kuo, C. H.; Suib, S. L. *ChemCatChem* **2013**, *5*, 920−930.

(36) Poyraz, A. S.; Kuo, C.-H.; Kim, E.; Meng, Y.; Seraji, M. S.; Suib, S. L. *Chem. Mater.* **2014**, *26*, 2803−2813.

(37) Biswas, S.; Poyraz, A. S.; Meng, Y.; Kuo, C.-H.; Guild, C.; Tripp, H.; Suib, S. L. *Appl. Catal., B* **2015**, *165*, 731−741.

(38) Poyraz, A. S.; Kuo, C.-H.; Biswas, S.; King'ondu, C. K.; Suib, S. L. *Nat. Commun.* **2013**, *4*, 2952.

(39) Wasalathanthri, N. D.; Poyraz, A. S.; Biswas, S.; Meng, Y.; Kuo, C.-H.; Kriz, D. A.; Suib, S. L. *J. Phys. Chem. C* **2015**, *119*, 1473−1482.

(40) Pahalagedara, L. R.; Poyraz, A. S.; Song, W.; Kuo, C.-H.; Pahalagedara, M. N.; Meng, Y.-T.; Suib, S. L. *Chem. Mater.* **2014**, *26*, 6613−6621.

(41) Song, W.; Poyraz, A. S.; Meng, Y.; Ren, Z.; Chen, S.-Y.; Suib, S. L. *Chem. Mater.* **2014**, *26*, 4629−4639.

(42) Kuo, C.-H.; Mosa, I. M.; Poyraz, A. S.; Biswas, S.; El-Sawy, A. M.; Song, W.; Luo, Z.; Chen, S.-Y.; Rusling, J. F.; He, J.; Suib, S. L. *ACS Catal.* **2015**, *5*, 1693−1699.

(43) Özacar, M.; Poyraz, A. S.; Genuino, H. C.; Kuo, C.-H.; Meng, Y.; Suib, S. L. *Appl. Catal., A* **2013**, *462*, 64−74.

(44) Genuino, H. C.; Dharmarathna, S.; Njagi, E. C.; Mei, M. C.; Suib, S. L. *J. Phys. Chem. C* **2012**, *116*, 12066.

(45) Sithambaram, S.; Kumar, R.; Son, Y.-C.; Suib, S. L. *J. Catal.* **2008**, *253*, 269−277.

(46) Johnson, C. D. *The Hammett Equation*; CUP Archive, 1973.

(47) Brown, H. C.; Okamoto, Y. *J. Am. Chem. Soc.* **1958**, *80*, 4979−4987.

(48) Poyraz, A. S.; Dag, O. m. *J. Phys. Chem. C* **2009**, *113*, 18596−18607.

(49) Huang, X.; Zheng, M.; Wang, Y. X.; Li, D. D.; Zhao, Y. J. *Adv. Mater. Res.* **2011**, *233*, 2904.

(50) Karimi, B.; Biglari, A.; Clark, J. H.; Budarin, V. *Angew. Chem., Int. Ed.* **2007**, *46*, 7210−7213.

(51) Largeron, M.; Chiaroni, A.; Fleury, M. B. *Chem. - Eur. J.* **2008**, *14*, 996−1003.

(52) Zheng, N.; Stucky, G. D. *Chem. Commun.* **2007**, *113*, 3862−3864.

(53) Doornkamp, C.; Ponec, V. . *J. Mol. Catal. A: Chem.* **2000**, *162*, 19−32.

(54) Martra, G.; Ocule, R.; Marchese, L.; Centi, G.; Coluccia, S. *Catal. Today* **2002**, *73*, 83−93.

(55) Helwani, Z.; Othman, M.; Aziz, N.; Kim, J.; Fernando, W. *Appl. Catal., A* **2009**, *363*, 1−10.

(56) Makwana, V. D.; Son, Y.-C.; Howell, A. R.; Suib, S. L. *J. Catal.* **2002**, *210*, 46−52.

(57) Introduction of 0.5 mmol of water into the reaction system gave a higher conversion (41%) than without adding water (30%) after 30 min of reaction